SUPER-RESOLUTION/SEGMENTATION OF 2D TRABECULAR BONE IMAGES BY A MUMFORD-SHAH APPROACH AND COMPARISON TO TOTAL VARIATION

Y.Li, A.Toma, B.Sixou, F.Peyrin

* CREATIS, CNRS UMR 5220, Inserm U630, INSA de Lyon, Universite de Lyon, F-69621
† ESRF,6 rue Jules Horovitz, F-38043, Grenoble Cedex France

ABSTRACT

The analysis of trabecular bone micro structure from *in-vivo* CT images is still limited due to insufficient spatial resolution. The goal of this work is to address both the problem of increasing the resolution of the image and of the segmentation of the bone structure. To this aim, we investigate the joint super-resolution/segmentation problem by an approach based on the Mumford-Shah model. The validation of the method is performed on blurred, noisy and down-sampled images. A comparison of the reconstruction results with the Total Variation regularization is showed.

Index Terms— Super-resolution/segmentation, Mumford-Shah, total variation, alternating minimization, 3D CT image, bone micro-architecture.

1. INTRODUCTION

The study of the trabecular bone micro-architecture is important in the diagnosis of osteoporosis because it is one of the determinant of bone strength [1]. This investigation remains difficult for *in-vivo* CT images because of the lack of resolution of the CT scanners compared with the trabeculae bone size. The bone structure analysis is based on the segmentation of the images to extract the bone architecture from the background. This segmentation is the first step to calculate the morphological or the topological parameters describing the bone micro-structure. New High Resolution peripheral Quantitative CT (HR-pQCT) devices with improved spatial resolution are now available to investigate the bone micro-architecture with *in-vivo* [2] measurements. After binarization, the quantitative parameters of trabecular bone architecture can be extracted since this technique provides images with a voxel size of 82 μm. Yet, the spatial resolution of the images is still too low because it remains close to the trabeculae size, and the segmentation step remains an issue. The aim of this work is to investigate joint super-resolution/segmentation methods to improve the trabecular bone analysis from *in-vivo* HR-pQCT images.

In image processing, the segmentation [3–5] and the super-resolution [6–9] problems have been much studied. However, in most cases these tasks are considered separately.

In previous works, we investigated methods to improve the quality of trabecular bone micro-CT images based on Total Variation regularization [11]. The images we considered having a quasi-binary structure, good results were obtained with single-image super-resolution. Results on experimental micro-CT images artificially deteriorated showed an improvement of the bone parameters. However, it is not clear which is the best regularization scheme for this inverse problem [10].

Meanwhile some non-convex regularizers have also been proposed recently [13, 14] since they may lead to better reconstruction results for some imaging applications than classical convex regularizers. It has also been suggested that solving joint segmentation/reconstruction problems based on the Mumford-Shah regularization functional leads to better reconstruction results than performing reconstruction and segmentation successively [15–17]. In detail, the Mumford-Shah functional has been firstly used for image denoising and segmentation problems for a forward operator A equal to the identity operator [18]. Recently, this functional has been used as a regularization term for linear and non linear problems [15,19–23]. Its regularization properties have been studied in detail and it has been shown that the Mumford-Shah regularization is stable for perturbations in the data [19].

In this work, we study the Mumford-Shah approach for the joint super-resolution/segmentation problem and detail the algorithm used to minimize the regularization functional. We also compare it to TV regularization. This paper is organized as follows. In the first section, we introduce the joint segmentation/super-resolution inverse problem and the Mumford-Shah regularization approach. Then, we present the results obtained with noisy micro-CT images of bone samples after simulating the effect of a loss of spatial resolution and degradation by noise.

2. SUPER-RESOLUTION/SEGMENTATION PROBLEM

2.1. The inverse problem formulation

The reconstruction of a 2D image with an improved resolution from a single low-resolution image is based on the direct problem of the image degradation. In our approach, we as-

978-0-9928-6265-7/16/$31.00 ©2016 IEEE

sume that the low-resolution image is obtained from the high-resolution image with a blurring followed by down-sampling, with some additional source of noise. The forward problem can be written as:

$$g = Af + n \tag{1}$$

where $g \in \mathbb{R}^N$ denotes the N-pixels low-resolution noisy image, and $f \in \mathbb{R}^{N'}$ denotes an $N' = N \times p^2$-pixels high-resolution image with super-resolution factor p in each dimension, $A : L_2(\Omega) \to L_2(\Omega)$ is the linear operator accounting for blurring followed by down-sampling defined on the bounded domain $\Omega \in \mathbb{R}^{N'}$ and n is the noise component. Our inverse problem is to recover the image f from the given degraded image g. It is an ill-posed problem, errors in the data will be magnified and this problem must be regularized. Stable solutions can be obtained by minimizing a regularization functional of the form:

$$\min_f \mu \|Af - g^\delta\|_2^2 + \mathcal{R}(f) \tag{2}$$

where $\mathcal{R}(f)$ is a regularization term which introduces some *a priori* knowledge on the solution. The first term enforces the fitting to the data. The regularization parameter μ controls the balance between the two terms of the regularization functional.

The images considered are quasi-binary and the problem can be understood as a joint segmentation/reconstruction problem. Recently, we investigated Total Variation(TV) schemes as a regularization term to solve this problem to obtain stable solutions [11]. The TV regularization term is defined as the L_1 norm of the gradient, $TV(f) = \int_\Omega |\nabla f(\mathbf{r})| d\mathbf{r}$, where $|\nabla f(\mathbf{r})|$ is the Euclidean norm of the gradient. The TV regularization method is well-known as a very effective way to recover edges of an image. The TV is convex and thus rather easy to minimize but the reconstruction may also benefit from non convex regularizers.

2.2. The Mumford-Shah type regularization

Let us introduce the Mumford-Shah regularization. It generalizes the Potts model presented in the [22], which is used at the second step of ADMM iteration described at next section, with an additional regularization term with the L_2 norm of the gradient. Let $SBV(\Omega)$ the set of special functions of Bounded Variation for which the Cantor part of the Total Variation is zero and $A : L_2(\Omega) \to L_2(\Theta)$ a continuous forward operator. The weak Mumford-Shah functional for $f \in SBV(\Omega)$ can be written:

$$MS(f) = \frac{\mu_1}{2}\|A(f) - g\|^2_{L^2(\Omega)} + \mu_2 \int_\Omega |\nabla f|^2 dx + \mathcal{H}(S_f) \tag{3}$$

where S_f is the jump set of the function f and ∇f the density of the Lebesgue integrable part of Df. The Hausdorff measure of the jump set is denoted as $\mathcal{H}(S_f)$. By minimizing the Mumford-Shah functional, it is possible to find the image f and its edges. Two regularization parameters μ_1 and μ_2 are introduced in the functional. The first term is a smoothing term. The second regularization term is the Hausdorff measure of the jump set S_f of the function f. This term induces a short and regular edge set. This regularization functional is expected to be very efficient to recover our quasi-binary image with a regular boundary curve. The existence of a solution for this functional and the regularization properties can be found in [19] for function f in $SBV(\Omega)$ and under some assumptions on the edge set S_f and the operator A.

The minimization of the Mumford-Shah functional is a difficult problem. Ramlau et al. have proposed level-set based minimization methods [15–17]. In [21], a good approximation of the Hausdorff measure for piecewise constant images is obtained with the discretization:

$$\sum_{s=1}^{S} \omega_s \|\nabla_{p_s} f\|_0 \tag{4}$$

where p_s are displacement vectors belonging to a neighborhood system, ω_s are nonnegative weights and $\nabla_{p_s} f = f(. + p) - f$, $\|\nabla_{p_s} f\|_0$ denotes the number of non zero entries of $\nabla_{p_s} f$. An efficient calculation of this regularization term by dynamic programming was proposed in [21].

2.3. An ADMM approach for the minimization

To solve the Mumford-Shah in this work, we propose an algorithm based on the alternating direction method of multipliers (ADMM). This method is among the state of the art method for minimizing regularization functional like TV [24–28]. To this aim, we have considered the classical following Lagrangian [25, 26] :

$$\begin{aligned} L(f, u, \mu_1, \mu_2, \beta, \lambda) =& \frac{\mu_1}{2}||Af - g||_2^2 + \mu_2||\nabla f||_2^2 \\ &+ ||\nabla u||_0 + \beta||f - u||_2^2 + < \lambda, f - u > \end{aligned}$$

where μ_1 and μ_2 are parameters balancing the data term and the regularization terms, $\lambda \in \mathbb{R}^{N'}$ is a Lagrange multiplier, β is a Lagrange parameter and u an auxiliary variable for the constraint. A saddle point of the Lagrangian is obtained with successive optimizations with respect to f,u and λ.

The ADMM iterates are the following:

1. *Update of f*

   $$Hf^{k+1} = \mu_1 A^t g + 2\beta u^k - \lambda^k$$

   with $H = \mu_1 A^t A + 2\beta - \mu_2 \triangle$, and where $\triangle$ is the Laplacian operator.

2. *Update of u*

   $$u_{k+1} \in arg\min_u \|\nabla u\|_0 + \lambda^k (f^{k+1} - u) + \beta \|f^{k+1} - u\|_2^2$$

which can be rewritten

$$u_{k+1} \in arg\min_u \|\nabla u\|_0 + \beta\|u - f^{k+1} - \frac{\lambda^k}{2\beta}\|_2^2 - \beta\|\frac{\lambda^k}{2\beta}\|_2^2$$

3. *Update of* λ

$$\lambda^{k+1} = \lambda^k - 2\beta(f^{k+1} - u^{k+1})$$

The step two of the algorithm is performed with a four neighborhood system and with the dynamic programming code given in [21].

3. NUMERICAL EXPERIMENTS

3.1. Simulation details

The tests were performed from experimental image of trabecular bone obtained from parallel-beam synchrotron micro-CT [29]. From these data, a 2D image with $N^2 = 328 \times 328$ pixels of size 20 μm was generated and considered as high-resolution ground truth image. The corresponding binarized ground truth is presented in Fig.1(a).

We blurred this high-resolution image with Gaussian point spread function with a standard deviation $\sigma_{blur} = 4.85$. The down-sampling rate was $p = 4$. A Gaussian noise with a standard deviation $\sigma = 1$ or $\sigma = 6$ was added to the blurred, under-sampled image. The generated image noted by g is shown in Fig.1(b).

During ADMM, we considered the convergence was achieved and the iterations were stopped if the relative change on the image satisfies $\frac{\|f_k - f_{k+1}\|_2}{\|f_k\|_2} < 2 * 10^{-2}$. The initial value of the Lagrangian multiplier λ is 0. The initial values of u and f are $A^t g$. For fixed regularization parameters, the β parameter was chosen to have the fastest decrease of the Lagrangian. In order to compare the regularization schemes, an extensive sweeping of the regularization parameters was performed.

Our methods have also been compared with regularization parameter chosen according to the Morozov discrepancy principle [10, 30, 31]. With the Morozov discrepancy principle, the regularization parameters are chosen such that the discrepancy term is equal to the known noise level δ on the observed data, so that the following equation holds, $\|Af(\mu_1, \mu_2) - g\| = \delta$, where $\delta = \|n\|_2$ is the noise level and $f(\mu_1, \mu_2)$ the reconstructed image for the parameters μ_1 and μ_2. The noise level is evaluated as $\delta^2 = N^2\sigma^2$. At the end of the optimization process the PSNR is calculated as: $PSNR = 10log_{10}\frac{(max(f^*) - min(f^*))^2}{||f^* - f||_2^2}$, where f^* is the high-resolution ground truth image and f is the super-resolution image. Then the binary images are obtained with the Otsu [32] threshold to calculate the DICE and bone surface (mm^2).

3.2. Results

Fig. 1 compares the binary reconstructed images obtained for $\sigma = 1$ with the two regularization methods, for an optimal choice of the regularization parameters and for parameters chosen with Morozov principle. The evolution of the data term for the Mumford-Shah approach as a function of the parameter μ_1 is displayed in Fig. 2 for $\mu_2 = 10^{-12}$ when the noise level $\sigma = 1$. This figure shows how the regularization parameter is determined according to the Morozov principle. The figures 3 and 4 independently present the evolution of PSNR and DICE with μ_1. Similar evolutions are obtained for $\sigma = 6$.

Table 1 and 2 compare TV and Mumford-Shah methods in terms of PSNR, DICE as well as bone surface for different noise levels. For the Mumford-Shah regularization, the optimal regularization parameters and the ones obtained with the Morozov principle are the same. For the TV regularization, there is a significant shift between the optimal parameter and the parameter determined with this discrepancy principle.

From these tables, we see that the Mumford-Shah method is very efficient for our reconstruction/segmentation problem. The TV methods gives better reconstruction results and the best structural parameters if the regularization parameters are chosen to maximize the PSNR, knowing the ground-truth. If the regularization parameters are chosen with the Morozov principle, the Mumford-Shah approach outperforms the TV based methods. In practical situations, where the ground truth image is not known, the Mumford-Shah regularization approach could be more efficient to perform the joint super-resolution/segmentation at the same time.

4. CONCLUSION

In this paper, we have proposed a super-resolution/segmentation method based on the Mumford-Shah regularization functional. We have compared the results, which are obtained with the TV regularization for the improvement of the quantification of the trabecular bone micro-structure on noisy, blurred, low-resolution images obtained from micro-CT volume, in terms of DICE, PSNR and bone surface. The better reconstruction results are obtained with the Mumford-Shah method if the parameters are chosen according to the Morozov principle even though ground truth is unknown. Preliminary studies with other images and noise levels seem to validate our conclusion. The method is thus promising to improve image quality and quantification.

5. REFERENCES

[1] E. Seeman and P. D. Delmas, "Bone quality-the material and structural basis of bone strength and fragility", *N. Engl. J. Med.*, vol. 354, no. 21, pp. 2250-2261, 2006.

[2] S. Boutroy, M. L. Bouxsein, F. Munoz and P. D. Delmas, "In vivo assessment of trabecular bone microarchitecture by high-

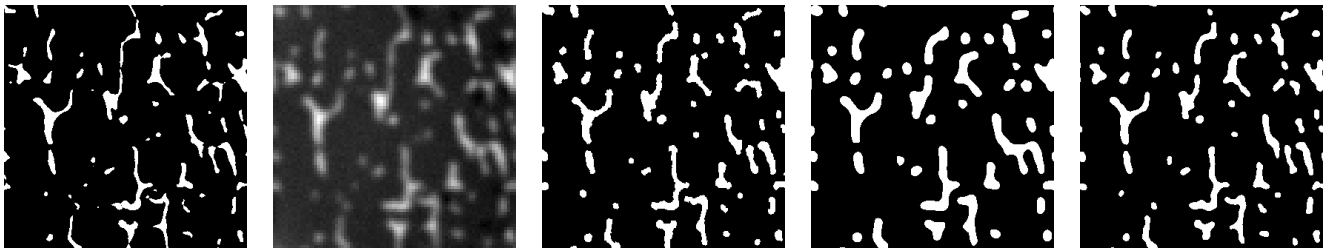

(a) Ground-truth image (b) Low resolution image (c) Mumford-Shah (c) TV with Morozov (e) TV without Morozov

Fig. 1. Comparison of super-resolution results, for a standard deviation of the noise $\sigma = 1$.

Table 1. Reconstruction results for Mumford-Shah, Total Variation, $\sigma = 1$

Regularization $\sigma = 1$	Parameter principle	PSNR	DICE	Bone Surface ref=3.94 (mm^2)
Mumford-Shah	with Morozov principle	21.89	0.80	5.16
	without Morozov principle	21.89	0.80	5.16
TV	with Morozov principle	20.00	0.70	6.36
	without Morozov principle	22.72	0.82	5.14

Table 2. Reconstruction results for Mumford-Shah, Total Variation, $\sigma = 6$

Regularization $\sigma = 6$	Parameter principle	PSNR	DICE	Bone Surface ref=3.94 (mm^2)
Mumford-Shah	with Morozov principle	18.75	0.68	5.42
	without Morozov principle	18.75	0.68	5.42
TV	with Morozov principle	17.28	0.54	4.33
	without Morozov principle	19.78	0.70	6.34

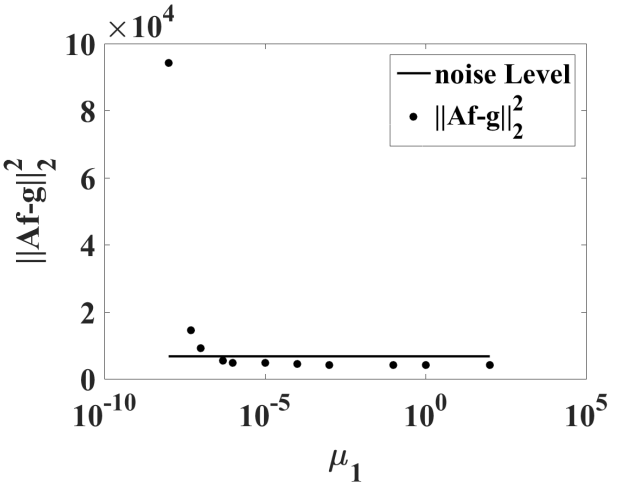

Fig. 2. Evolution of the data term $||Af - g||_2^2$ as a function of μ_1 for the Mumford-Shah regularization and noise level δ^2 for $\sigma = 1$

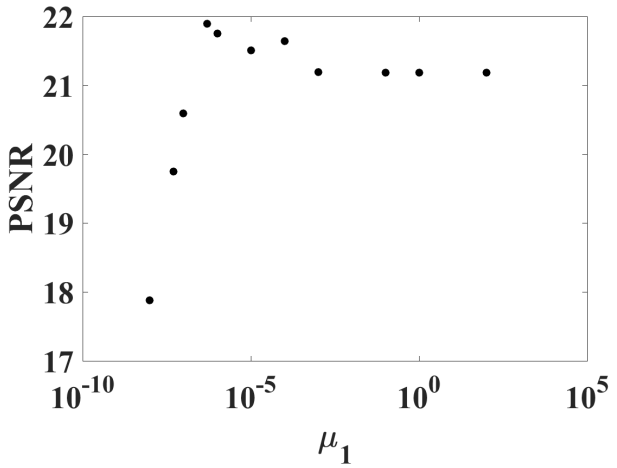

Fig. 3. Evolution of the PSNR as a function of μ_1 for the Mumford-Shah regularization and $\sigma = 1$.

resolution peripheral quantitative computed tomography", *J. Clin. Endocrinol. Metab.*, vol. 90, no. 12, pp. 6508-15, 2005.

[3] T. F. Chan and L. Vese, "Active contours without edges", *IEEE Trans.Image Process.*, vol. 10, 266-277, 2001.

[4] D. Cremers, M. Rousson and R. Deriche, "A review of stastistical approaches to level-set segmentation: integrating color, texture, motion and shape", *Int.J.Comput.Vis.*, vol. 72, 195-215, 2007.

[5] T. Goldstein, X. Bresson and S. Osher, "Geometric application of the split Bregman method:segmentation and surface reconstruction", *Int.J.Comput.Vis.*, vol. 45, 272-93, 2010.

[6] S. Chaudhuri, "Super-resolution Imaging", Norwell, MA:Kluwer, 2001.

[7] S. C. Park, M. K. Park and M. G. Kang "Super-resolution image reconstruction: a technical overview", *IEEE Signal Process. Mag.*, vol. 20, no. 3, pp. 21-36, 2003.

[8] S. D. Babacan, R. Molina and A. K. Katsaggelos, "Total Variation super resolution using a variational approach", *Proc. Int. Conf. Image Process.*, 641-644, 2008.

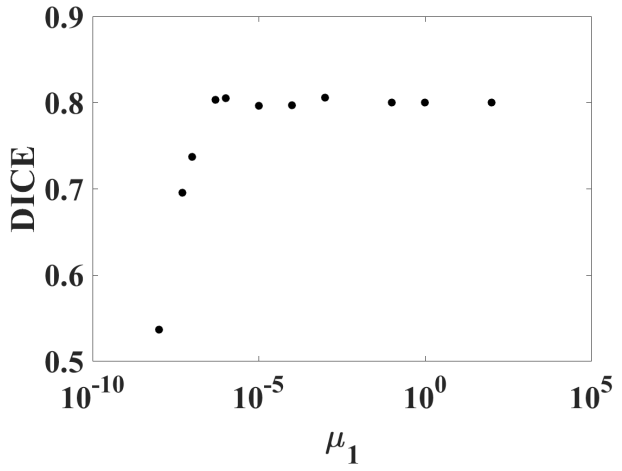

Fig. 4. Evolution of DICE as a function of μ_1 for the Mumford-Shah regularization and $\sigma = 1$.

[9] Z. Ren, C. He and Q. Zhang, "Fractional order Total Variation regularization for image super-resolution", *Signal Process.*, vol. 93, 2408-2421, 2013.

[10] A. Toma, B. Sixou and F. Peyrin "Iterative choice of the optimal regularization parameter in TV image restoration", *Inverse Problems and Imaging* , vol. 9, 1171-1191, 2015.

[11] A. Toma, L. Denis, B. Sixou, J. B. Pialat, F. Peyrin "Total Variation super-resolution for 3D trabecular bone micro-structure segmentation", *Eusipco* pp.2220-2224, 2014.

[12] L. I. Rudin, S. Osher and E. Fatemi, "Nonlinear total variation based noise removal algorithms", *Phys.D*, vol. 60, pp. 259-268, 1992.

[13] R. Chartrand, "Exact reconstruction of sparse signals via nonconvex minimization", *IEEE Signal Processing Letters*, vol. 14, 707-710, 2007.

[14] E. Candes, M. Walkin and S. Boyd *Enhancing sparsity by reweighted l_1 minimization* , Journal of Fourier Analysis and Applications, vol.14, 877-905, 2008.

[15] R. Ramlau and W. Ring, "A Mumford-Shah level-set approach for the inversion and segmentation of X-ray tomography data", *Journal of Computational Physics* , vol.221, 539-557, 2007.

[16] E. Klann, "A Mumford-Shah-like method for limited data tomography with an application to electron tomography", *SIAM J.Imaging Sci* , 4, 1029-1048, 2011.

[17] E. Klann and R. Ramlau, "Regularization properties of Mumford-Shah type functionals with perimeter and norm constraints for linear ill-posed problems", *SIAM J.Imaging Sci*, 6, 413-436, 2013.

[18] D. Mumford and J. Shah "Optimal approximations by piecewise smooth functions and associated variational problems", *Communications on Pure and Applied Mathematics* , vol.42, 577-685, 1989.

[19] M. Jiang, P. Maass and T. Page, "Regularizing properties of the Mumford-Shah functional for imaging applications", *Inverse Problems* , vol.30, 035007, 2014.

[20] R. Ramlau and W. Ring, "Regularization of ill-posed Mumford-Shah models with perimeter penalization", *Inverse Problems* , vol.26, 115001, 2010.

[21] M. Storath, A. Weinmann, J. Frikel and M. Unser "Joint image reconstruction and segmentation using the Potts model", *Inverse Problems*, vol.31, 025003, 2015.

[22] M. Storath, A. Weinmann and L. Demaret "Jump-sparse and sparse recovery using Potts functional", *IEEE Transactions on Signal Processing* , vol.62, 3654-3666, 2014.

[23] A. Weinmann, M. Storath and L. Demaret "The L^1-Potts functional for robust jump-sparse reconstruction", *SIAM Journal on Numerical Analysis*, vol.53, 644-673, 2012.

[24] J. Yang, W. Yin, Y. Zhang and Y. Wang, "A fast algorithm for edge-preserving variational multichannel image restoration", *SIAM J. Imaging Sci.*, vol.2, pp.569-592, 2008.

[25] M. Afonso, J. Bioucas-Dias and M. Figueiredo, "Fast image recovery using variable splitting and constrained optimization", *IEEE Trans. Image Process.*, vol.19, pp. 2345-2356, 2010.

[26] M. Afonso, J.Bioucas-Dias and M.Figueiredo, *An augmented Lagrangian approach to the constrained optimization formulation of imaging inverse problems*, IEEE Trans. Image Process., 20 , 681-695, 2011.

[27] MK. Ng, P. Weiss and X. Yuan, "Solving constrained total-variation image restoration and reconstruction problems via alternating direction mehthods", *SIAM J. Sci. Comput.*, vol.32, pp. 2710-2736, 2010.

[28] Y. Wang, J. Yang, W. Yin and Y. Zhang, *A new alternating minimization algorithm for total variation image reconstruction*, SIAM Journal on Imaging Sciences, vol.1, 248-272, 2008.

[29] M. Salome, F. Peyrin, P. Cloetens, C. Odet, A. M. Laval-Jeantet, J. Baruchel and P. Spanne, "A synchrotron radiation microtomography system for the analysis of trabecular bone samples", *Med. Phys.*, vol.26, no. 10, pp. 2194-2204, Oct. 1999

[30] V. A. Morozov, "Methods for Solving Incorrectly Posed Problems", New York: Springer-Verlag, 1984.

[31] K. Kunisch and J. Zou, *Iterative choices of regularization parameters in linear inverse problems*, Inverse Problems, 14, 1247-1264, 1998.

[32] N. Otsu *A threshold selection method from gray-level histograms*, IEEE Trans.Sys., Man.Cyber, 9, 77-92, 1979.